NON-UNIFORM TRANSMISSION LINE ULTRA-WIDEBAND WILKINSON POWER DIVIDER

Khair Shamaileh[1, *], Mohammad Almalkawi[1], Vijay Devabhaktuni[1], Nihad Dib[2], Bassem Henin[3], and Amin Abbosh[3]

[1]Electrical Engineering & Computer Science Department, University of Toledo, Toledo, OH 43606, USA

[2]Electrical Engineering Department, Jordan University of Science and Technology, Irbid 22110, Jordan

[3]School of ITEE, University of Queensland, St Lucia, QLD 4072, Australia

Abstract—We propose a technique with clear guidelines to design a compact planar Wilkinson power divider (WPD) for ultra-wideband (UWB) applications. The design procedure is accomplished by replacing the uniform transmission lines in each arm of the conventional power divider with varying-impedance profiles governed by a truncated Fourier series. Such non-uniform transmission lines (NTLs) are obtained through the even mode analysis, whereas three isolation resistors are optimized in the odd mode circuit to achieve proper isolation and output ports matching over the frequency range of interest. For verification purposes, an in-phase equal split WPD is designed, simulated, and measured. Simulation and measurement results show that the input and output ports matching as well as the isolation are below $-10\,\mathrm{dB}$, whereas the transmission parameters are in the range of $(-3.2\,\mathrm{dB}, -4.2\,\mathrm{dB})$ across the 3.1 GHz–10.6 GHz band.

1. INTRODUCTION

Ultra-wideband frequency spectrum finds several key applications in many modern and emerging technologies, such as tactical and strategic communications [1], through-the-wall imaging [2], medical treatments [3, 4], and high data rate transmission [5, 6]. Consequently,

the need for microwave components that support such a range of frequencies is of utmost importance. Among various RF devices, the Wilkinson power divider (WPD), invented by E. Wilkinson [7], is a passive component that gained much interest in the literature due to its capability to achieve isolation between the output ports while maintaining a matched condition at all ports. Those significant characteristics qualified its adoption in countless front-end microwave subsystems. In [8], a reduced-size UWB power divider was proposed by implementing the transmission lines of a two-stage WPD using bridged T-coils. However, the accompanied complexity in the design and fabrication is a major drawback in such an approach. Bialkowski and Abbosh proposed a compact UWB out-of-phase uniplanar power divider formed by a slotline and a microstrip line T-junction along with wideband microstrip to slotline transitions [9]. A miniaturized three-way power divider with ultra-wideband behavior was presented in [10] by utilizing broadside coupling via multilayer microstrip/slot transitions of elliptical shape. Tapered line transformers, which exhibit almost constant input impedance over a wide range of frequencies, were incorporated in the design of an UWB divider [11]. Nevertheless, the resulting circuitry area was comparatively large. Different kinds of stubs such as open stubs [12], delta stubs [13], and radial stubs [14] were introduced as an approach in designing modified WPDs with extended bandwidth. As such, extra transmission lines were integrated in the proposed techniques.

In this paper, compact UWB WPD based on non-uniform transmission lines is proposed. The soul of the design approach depends mainly on the even/odd mode circuits, which results in the replacement of the uniform microstrip arms of the conventional power divider by variable-width impedance profiles. Furthermore, three isolation resistors are optimized and uniformly mounted between both arms to maintain an acceptable isolation and output ports' matching over the entire band.

The article organization is as follows: Section 2 discusses the design procedure of the proposed UWB NTLs power divider. Simulation and measurement results of a designed example are presented in Section 3. Finally, conclusions and remarks are given in Section 4.

2. ULTRA-WIDEBAND WPD DESIGN

A schematic diagram of the proposed device is shown in Fig. 1, which presents the modified UWB equal-split WPD. Each uniform impedance branch in the conventional divider is replaced by a single
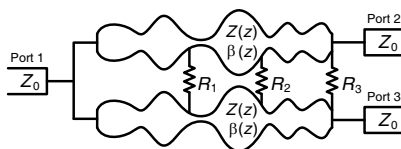
Figure 1. Schematic diagram for the proposed NTLs ultra-wideband WPD.
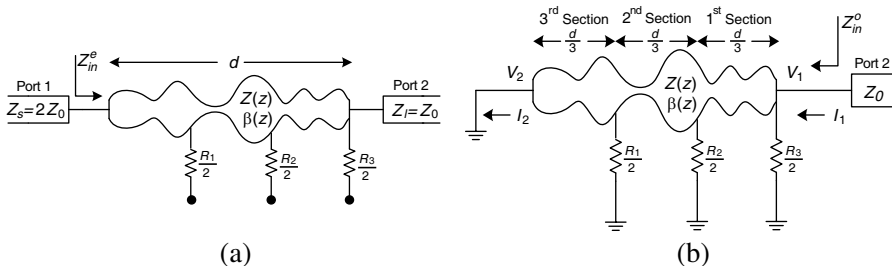
Figure 2. Proposed non-uniform WPD: (a) even-mode; and (b) odd-mode circuits.

NTL transformer to achieve UWB operation.

Figure 2 illustrates the corresponding even and odd mode circuits. In Section 2.1 (even mode analysis), the design of the NTLs is presented; whereas in Section 2.2 (odd mode analysis), the values of the isolation resistors are derived to meet acceptable output ports' isolation and matching.

2.1. Even Mode Analysis

The even mode equivalent circuit is shown in Fig. 2(a), which presents a typical NTL of length d with a varying characteristic impedance $Z(z)$ and propagation constant $\beta(z)$ that matches a source impedance Z_s to a load impedance Z_l. In our case, $Z_s = 2Z_0$ and $Z_l = Z_0$. The isolation resistors $R_i/2$ ($i = 1, 2, 3$), due to the symmetric excitation at the two output ports, are terminated with an open circuit. The NTL is designed by enforcing the magnitude of the reflection coefficient $|\Gamma|$ to be zero (or very small) over the frequency range 3.1 GHz–10.6 GHz. The magnitude of the reflection coefficient at the input port can be expressed in terms of Z_{in}^e shown in Fig. 2(a), where Z_{in}^e can be calculated after obtaining the $ABCD$ parameters of the NTL. Those $ABCD$ parameters are found by subdividing such a transformer into K uniform electrically short segments each with length of Δz. It is worth

to point out here that the number of the uniform short sections K is chosen to be 50. The $ABCD$ matrix of the whole NTL transformer is obtained by multiplying the $ABCD$ parameters of each section as follows [15]:

$$\begin{bmatrix} A & B \\ C & D \end{bmatrix}_{Z(z)} = \begin{bmatrix} A_1 & B_1 \\ C_1 & D_1 \end{bmatrix} \cdots \begin{bmatrix} A_i & B_i \\ C_i & D_i \end{bmatrix} \cdots \begin{bmatrix} A_K & B_K \\ C_K & D_K \end{bmatrix}. \quad (1)$$

where the $ABCD$ parameters of the ith segment are [15]:

$$A_i = D_i = \cos(\Delta\theta), \tag{2a}$$

$$B_i = Z^2((i-0.5)\Delta z)C_i = jZ((i-0.5)\Delta z)\sin(\Delta\theta), \ \ i = 1, 2, \ldots, K, \tag{2b}$$

$$\Delta\theta = \frac{2\pi}{\lambda}\Delta z = \frac{2\pi}{c}f\sqrt{\varepsilon_{eff}}\Delta z. \tag{2c}$$

The effective dielectric constant, ε_{eff}, of each section is calculated using the well-known microstrip line formulas given in [15]. Then, the normalized non-uniform profile of the characteristic impedance $Z(z)$, written in terms of a truncated Fourier series, is considered [16]:

$$\ln\left(\frac{Z(z)}{Z_c}\right) = c_0 + \sum_{n=1}^{N}\left[a_n\cos\left(\frac{2\pi nz}{d}\right) + b_n\sin\left(\frac{2\pi nz}{d}\right)\right]. \tag{3}$$

where Z_c, which equals $(Z_sZ_l)^{0.5}$, is the characteristic impedance of the conventional WPD arm. Thus, an optimum designed NTL has its reflection coefficient magnitude over the frequency range (3.1 GHz–10.6 GHz), with an increment of Δf, as close as possible to zero. Therefore, the optimum values of the Fourier coefficients can be obtained through minimizing the following error function [17]:

$$\text{Error}_{in} = \max\left(E_{f_1}^{in}, \ldots, E_{f_j}^{in} \ldots, E_{f_m}^{in}\right), \tag{4}$$

where

$$E_{f_j}^{in} = \left|\Gamma_{in}(f_j)\right|^2, \tag{5a}$$

$$\Gamma_{in}(f_j) = \frac{Z_{in}^e(f_j) - Z_s}{Z_{in}^e(f_j) + Z_s}, \tag{5b}$$

$$Z_{in}^e(f_j) = \frac{A(f_j)Z_l + B(f_j)}{C(f_j)Z_l + D(f_j)}. \tag{5c}$$

Moreover, the error function in (4) should be restricted by some constraints such as easy fabrication and physical matching, as follows [16]:

$$\bar{Z}_{\min} \leq \bar{Z}(z) \leq \bar{Z}_{\max}. \tag{6a}$$

$$\bar{Z}(0) = \bar{Z}(d) = 1. \tag{6b}$$

To solve the above bound-constrained non-linear minimization problem, a trust-region-reflective algorithm [18] is adopted, which has strong convergence properties.

2.2. Odd Mode Analysis

The odd-mode analysis is carried out to obtain the resistors' values needed to achieve the optimum output ports isolation and matching conditions. Fig. 2(b) shows the equivalent odd-mode circuit of the proposed divider [19], where the asymmetric excitation of the output ports results in terminating each $R_i/2$ resistor with a short circuit.

Once the optimum values of the Fourier coefficients are determined by following the procedure described in Section 2.1, the NTL transformer will be subdivided into 3 sections, and the $ABCD$ matrix for each section is calculated employing (1) and (2). Then, the total $ABCD$ matrix of the whole network shown in Fig. 2(b) can be calculated as follows [20]:

$$[ABCD]_{\text{Total}} = [ABCD]_{\frac{R_3}{2}} \cdot [ABCD]_{\text{1st Section}} \cdot [ABCD]_{\frac{R_2}{2}}$$
$$\cdot [ABCD]_{\text{2nd Section}} \cdot [ABCD]_{\frac{R_1}{2}} \cdot [ABCD]_{\text{3rd Section}} \quad (7)$$

It should be pointed out here that the isolation resistors are distributed uniformly (a resistor every $d/3$ distance) along the NTL transformer. Finally, and as illustrated in Fig. 2(b), the following equation can be written:

$$\begin{bmatrix} V_1 \\ I_1 \end{bmatrix} = \begin{bmatrix} A & B \\ C & D \end{bmatrix}_{\text{Total}} \begin{bmatrix} V_2 \\ I_2 \end{bmatrix}. \quad (8)$$

Setting V_2 in (8) to zero, and solving for $\frac{V_1}{I_1}$, one obtains:

$$\frac{V_1}{I_1} = \frac{B}{D} = Z_{in}^o. \quad (9)$$

For perfect output port matching, the following condition should be satisfied:

$$\Gamma_{out}(f_j) = \frac{Z_{in}^o(f_j) - Z_0}{Z_{in}^o(f_j) + Z_0}. \quad (10)$$

where f_j ($j = 1, 2, \ldots, m$) denotes the frequencies at which (10) is calculated. In the context of this article, Δf is set to 0.5 GHz. So, for a perfect output ports matching over the UWB range, the following error should be minimized:

$$\text{Error}_{out} = \max\left(E_{f_1}^{out}, \ldots, E_{f_j}^{out} \ldots, E_{f_m}^{out} \right), \quad (11a)$$

where

$$E_{f_j}^{out} = |\Gamma_{out}(f_j)|^2 . \tag{11b}$$

This optimization problem is solved keeping in mind that R_1, R_2, and R_3 are the optimization variables to be determined.

3. SIMULATION AND EXPERIMENTAL RESULTS

In this section, based on the design procedure provided in Section 2, a design example of an UWB power divider is presented taking into account a characteristic impedance of $50\,\Omega$ and a Rogers RO4003C substrate with a relative permittivity of 3.55, a thickness of $0.813\,\text{mm}$, and a loss tangent of 0.0027. The length of each NTL arm of the proposed WPD is set to $10\,\text{mm}$. The optimized Fourier coefficients of the designed nonuniform UWB power divider arm are given in Table 1; whereas Fig. 3 shows the corresponding variable impedance profile.

Table 1. Fourier coefficients for the variable impedance profile in the UWB WPD design.

| c_0	a_1	a_2	a_3	a_4	a_5	b_1	b_2	b_3	b_4	b_5
0.0191	0.0090	0.1335	0.0177	0.2015	0.1120	-0.4754	0.0733	-0.0701	0.1181	-0.1387
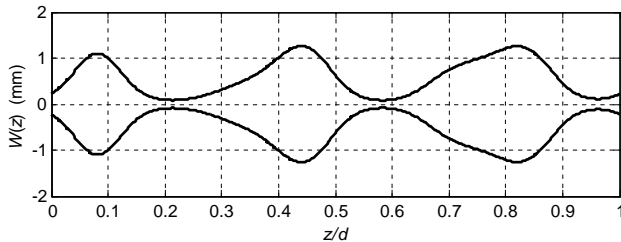
Figure 3. Optimized nonuniform UWB WPD arm.

A photograph of the fabricated divider is shown in Fig. 4. It is worth mentioning that the optimum values of the isolation resistors R_1, R_2, and R_3 are found to be $150\,\Omega$, $301\,\Omega$, and $133\,\Omega$, respectively.

Figure 5 illustrates the resulting simulated and measured scattering parameters. The simulation results were obtained using HFSS [12], which is a finite element method-based full-wave EM simulator, while the experimental ones were obtained using an HP8510 VNA.
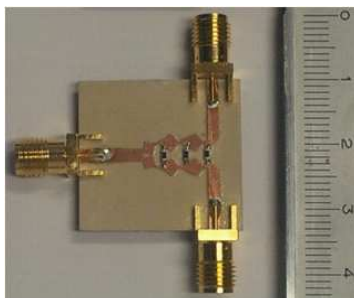
Figure 4. A photograph of the fabricated UWB non-uniform WPD.
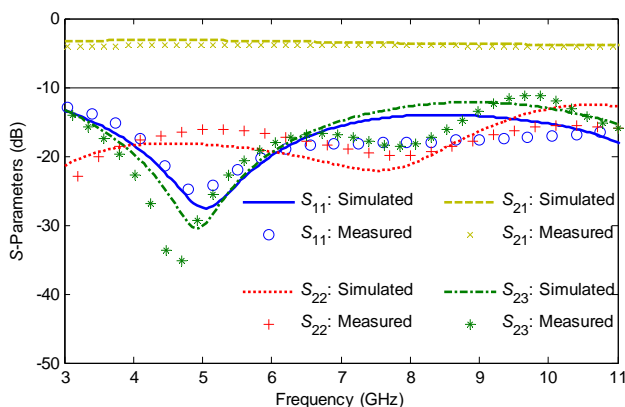
Figure 5. Simulated and measured S-parameters of the proposed UWB non-uniform WPD.

As shown in Fig. 5, the simulation and measurement results of the input and output ports match parameters S_{11} and S_{22} (which is equal to S_{33}), respectively, as well as the isolation parameter S_{23} are below -10 dB over the 3.1–10.6 GHz frequency band. Moreover, the simulated transmission parameter S_{21} is in the range of -3.2 dB to -3.8 dB, whereas the measured values of the same parameter ranges between -3.2 dB to -4.2 dB over the frequency range of interest. Such results are in proximity to the theoretical value of -3 dB. The small discrepancies between the simulations and measurements are thought to be due to the fabrication process and measurement errors (e.g., not taking the modeling of the SMA connectors into account). Fig. 6 shows the measured amplitude and phase imbalance between the two output ports of the proposed equal-split in-phase UWB divider.

The measured phase imbalance is less than $\pm 10°$ over the

entire design frequency range. Furthermore, the obtained amplitude imbalance is around $\pm 0.1\,\text{dB}$ over the $3.1\,\text{GHz}$–$10.6\,\text{GHz}$ band proving the excellent degree of symmetry of the implemented structure. Fig. 7 depicts the simulated and measured group delay responses of the designed WPD.

Both results are almost flat over the UWB range and less than $0.2\,\text{ns}$ with a mismatch thought to be due to the inhomogeneous

**Table 2.** Comparison between this work and different previous proposed designs.

	Arm length (mm)	S-Parameters over 3.1–10.6 GHz (dB)	Design approach/ Fabrication technology
This work	10	S_{11} $[-28, -14]$ S_{22} $[-22, -13]$ S_{23} $[-30, -13]$ S_{21} $[-3.8, -3.2]$	- Fourier-based transmission lines - Single-layer substrate - No stubs are incorporated
Ref. [9]	20	S_{11} $[-19, -10]$ S_{22} $[-12, -10]$ S_{23} $[-10, -7]$ S_{21} $[-4.1, -3.8]$	- Slotline and two arms of a microstrip T-junction - Built on two-layer substrate - No stubs are incorporated
Ref. [11][*]	29.65	S_{11} $[-35, -19]$ S_{22} $[-40, -6]$ S_{23} $[-48, -7]$ S_{21} $[-3.3, -3.1]$	- Tapered lines transformer - Single-layer substrate - No stubs are incorporated
Ref. [12]	24	S_{11} $[-25, -10]$ S_{22} $[-40, -12]$ S_{23} $[-25, -10]$ S_{21} $[-4.2, -3.1]$	- Stub-loaded two-section microstrip - Single-layer substrate - stubs incorporated in the design
Ref. [13]	6.5	S_{11} $[-45, -14]$ S_{22} $[-55, -14]$ S_{23} $[-45, -10]$ S_{21} $[-4.1, -3.2]$	- Microstrip loaded with stubs - Single-layer substrate - Delta stubs incorporated
Ref. [14]	7	S_{11} $[-50, -18]$ S_{22} $[-20, -12]$ S_{23} $[-42, -12]$ S_{21} $[-3.5, -3.1]$	- Microstrip loaded with stubs - Single-layer substrate - Butterfly radial stubs incorporated

[*] The three isolation resistors case is taken in this comparison.
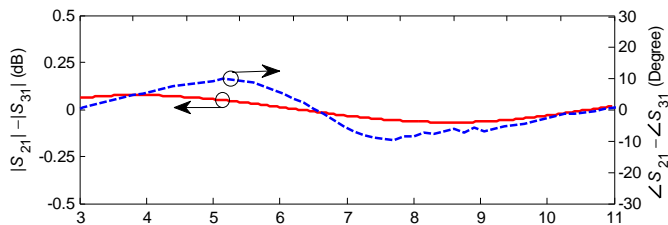
Figure 6. Measured amplitude and phase imbalance of the proposed UWB divider.
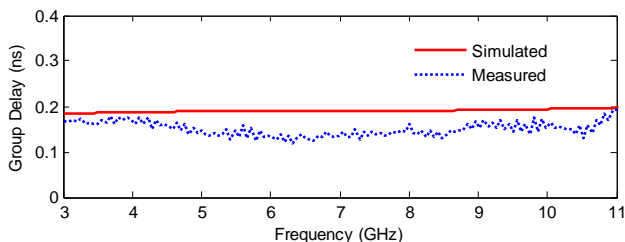
Figure 7. Simulated and measured group delay of the proposed UWB divider.

substrate material used in this project (i.e., a horizontal dielectric constant different than a vertical dielectric constant). Table 2 shows a comparison between our proposed design and other UWB Wilkinson power dividers presented in [9] and [11–14] taking into consideration size, electrical performance, design approach, and fabrication technology.

4. CONCLUSION

In this paper, a general design of an ultra-wideband WPD incorporating Fourier-based impedance-varying profiles is presented. The design of the ultra-wideband NTLs was obtained from the even mode analysis of the WPD, whereas three isolation resistors were calculated through the odd mode circuit. For verification purposes, an equal-split UWB power divider was designed, simulated, and measured. The good agreement between simulation and measurement results over the 3.1–10.6 GHz frequency range proves the validity of the design procedure. The differences between simulated and experimental results could be due to the fabrication process, the effect of the connectors, and measurement errors.

ACKNOWLEDGMENT

REFERENCES

1. Fontana, R., A. Ameli, E. Richley, L. Beard, and D. Guy, "Recent advances in ultra-wideband communications systems," *Proc. of IEEE Conf. on Ultra-wideband Sys. and Tech.*, 129–133, Baltimore, USA, May 2002.
2. Venkatasubramanian, V., H. Leung, and X. Liu, "Chaos UWB radar for through-the-wall imaging," *IEEE Trans. Image Process.*, Vol. 18, No. 6, 1255–1265, Jun. 2009.
3. Bialkowski, M. E., Y. Wang, and A. Abbosh, "UWB microwave mono-pulse radar system for breast cancer detection," *Proc. 4th Int. Conf. Signal Process. and Comm. Sys.*, 1–4, Gold Coast, Qld., Australia, Dec. 2010.
4. Ireland, D., A. Abbosh, M. Bialkowski, and E. Miller, "Study on optimal bandwidth for microwave breast imaging," *Proc. 7th Int. Conf. Intelligent Sensors, Sensor Networks and Information Processing*, 21–24, Adelaide, Australia, Dec. 2011.
5. Kshetrimayum, R., "An introduction to UWB communication systems," *IEEE Potentials*, Vol. 28, No. 2, 9–13, Mar.–Apr. 2009.
6. Yang, L. and G. B. Giannakis, "Ultra-wideband communications: An idea whose time has come," *IEEE Signal Process. Mag.*, Vol. 21, No. 6, 26–54, Nov. 2004.
7. Wilkinson, E., "An N-way hybrid power divider," *IRE Trans. Microw. Theory Technol.*, Vol. 8, 116–118, 1960.
8. Lin, Y.-S. and J.-H. Lee, "Miniature ultra-wideband power divider using bridged T-coils," *IEEE Microw. Wireless Compon. Lett.*, Vol. 22, No. 8, 391–393, Aug. 2012.
9. Bialkowski, M. and A. Abbosh, "Design of a compact UWB out-of-phase power divider," *IEEE Microw. Wireless Compon. Lett.*, Vol. 17, No. 4, 289–291, Apr. 2007.
10. Abbosh, A., "A compact UWB three-way power divider," *IEEE Microw. Wireless Compon. Lett.*, Vol. 17, No. 8, 598–600, Aug. 2007.

11. Chiang, C.-T. and B.-K. Chung, "Ultra-wideband power divider using tapered line," *Progress In Electromagnetics Research*, Vol. 106, 61–73, 2010.

12. Ou, X.-P. and Q.-X. Chu, "A modified two-section UWB Wilkinson power divider," *Int. Conf. on Microw. and Millimeter Wave Tech.*, 1258–1260, Vol. 3, Apr. 2008.

13. Zhou, B., H. Wang, and W.-X. Sheng, "A modified UWB Wilkinson power divider using delta stub," *Progress In Electromagnetics Research Letters*, Vol. 19, 49–55, 2010.

14. Zhou, B., H. Wang, and W.-X. Sheng, "A novel UWB Wilkinson power divider," *Proc. 2nd Int. Inform. Sci. Eng. Conf.*, 1763–1765, Hangzhou, China, Dec. 2010.

15. Pozar, D., *Microwave Engineering*, 3rd Edition, Wiley, New York, 2005.

16. Khalaj-Amirhosseini, M., "Wideband or multiband impedance matching using microstrip non-uniform transmission lines," *Progress In Electromagnetics Research*, Vol. 66, 15–25, 2006.

17. Shamaileh, K. and N. I. Dib, "Design of compact dual-frequency Wilkinson power divider using non-uniform transmission lines," *Progress In Electromagnetics Research C*, Vol. 19, 37–46, 2011.

18. Li, Y., "Centering, trust region, reflective techniques for nonlinear minimization subject to bounds," Technical Report 93-1385, Cornell University, NY, USA, Sep. 1993.

19. Shamaileh, K., A. Qaroot, N. Dib, and A.-F. Sheta, "Design and analysis of multifrequency Wilkinson power dividers using non-uniform transmission lines," *Int. J. RF and Microwave Comp. Aid. Eng.*, Vol. 21, 526–533, Sep. 2011.

20. Shamaileh, K., N. Dib, and A. Abbosh "Analysis and design of ultra-wideband unequal-split Wilkinson power divider using tapered lines transformers," *Electromagnetics*, Vol. 32, No. 7, 426–437, 2012.

21. ANSYS-High Frequency Structure Simulator (HFSS), Ansys, Inc., Canonsburg, PA, 2011.